NeuroImage 208 (2020) 116455

Contents lists available at ScienceDirect

NeuroImage

journal homepage: www.elsevier.com/locate/neuroimage

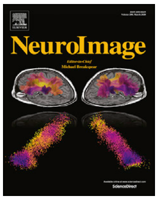

Interhemispheric auditory connectivity requires normal access to sound in both ears during development

Daniel A. Smieja [a,b,*], Benjamin T. Dunkley [b,c], Blake C. Papsin [d], Vijayalakshmi Easwar [b], Hiroshi Yamazaki [b], Michael Deighton [b], Karen A. Gordon [b,d]

[a] *Institute of Biomaterials and Biomedical Engineering, The University of Toronto, Toronto, ON, Canada*
[b] *Neurosciences and Mental Health, The Hospital for Sick Children, Toronto, ON, Canada*
[c] *Department of Diagnostic Imaging, The Hospital for Sick Children, Toronto, Canada*
[d] *Otolaryngology – Head & Neck Surgery, The Hospital for Sick Children, Toronto, ON, Canada*

ARTICLE INFO

Keywords:
EEG
Auditory pathways
Binaural hearing
Functional connectivity
Sensorineural hearing loss

ABSTRACT

Despite early bilateral cochlear implantation, children with congenital deafness do not develop accurate spatial hearing; we thus asked whether auditory brain networks are disrupted in these children. EEG responses were evoked unilaterally and bilaterally in 13 children with normal hearing and 16 children receiving bilateral cochlear implants simultaneously. Active cortical areas were estimated by the Time Restricted Artifact and Coherent source Suppression (TRACS) beamformer and connected cortical areas were identified by measuring coherence between source responses. A whole-brain analysis of theta band coherence revealed the strongest connections between the temporal areas in all conditions at early latencies. Stronger imaginary coherence in activity between the two auditory cortices to bilateral than unilateral input was found in children with normal hearing reflecting facilitation in the auditory network during bilateral hearing. The opposite effect, depressed coherence, was found during bilateral stimulation in children using cochlear implants. Children with cochlear implants also showed a unique auditory network in response to bilateral stimulation which was marked by increased connectivity between occipital and frontal areas. These findings suggest that cortical networks for sound processing are normally facilitated by bilateral input but are disrupted in children who hear through two independent cochlear implants. Efforts to improve hearing in children with congenital deafness must thus include corrections to potential mismatches in bilateral input to support brain development.

1. Introduction

Whereas previous studies have assessed the development of responses in left and right auditory cortices (Easwar et al., 2017), the present study sought to identify the cortical networks involved in binaural versus unilateral hearing and asked whether these functional connections remained compromised in children with deafness despite early access to bilateral cochlear implantation.

1.1. *Providing bilateral hearing in children who are profoundly deaf*

Recommendations to provide bilateral hearing during early life are based on evidence of cross-modal reorganization of auditory cortices (Lomber et al., 2010; Sharma et al., 2015) and aural preference which develops in the presence of asymmetric hearing in childhood (Gordon et al., 2015). Bilateral hearing provides the basis for spatial hearing which is needed to detect and discern sounds from all directions (Hawley et al., 2004) and is best promoted in children with congenital deafness by electrical stimulation of both auditory nerves with bilateral cochlear implants (CIs).

Providing bilateral CIs can be highly effective at promoting age-appropriate speech and language development (Wie, 2010) and cortical representation from both ears (Gordon et al., 2013). Expected cortical specialization (right hemispheric dominance to non-speech sounds) (Zatorre et al., 2002) also emerges in children receiving early access to bilateral cochlear implants unlike children who hear with a single implant (Easwar et al., 2017). Spatial hearing in children using bilateral cochlear implants remains abnormal (Litovsky and Gordon, 2016; Cullington et al., 2017), which means that they still struggle to hear in many situations. These ongoing challenges are likely related to

---

* Corresponding author. Institute of Biomaterials and Biomedical Engineering, The University of Toronto, Toronto, ON, Canada.
E-mail address: daniel.smieja@mail.utoronto.ca (D.A. Smieja).

https://doi.org/10.1016/j.neuroimage.2019.116455
Received 22 July 2019; Received in revised form 21 November 2019; Accepted 9 December 2019

the deterioration of neural responses to binaural input shown in animal models of congenital deafness (Tillein et al., 2016) and reflect the inability of present auditory devices to correct these deficits.

1.2. Disruption of cortical connectivity in childhood deafness

Congenital deafness has widespread structural and functional effects on the cortical auditory system (Review: Butler and Lomber, 2013), which are likely to change the cortical network (or connectome) involved in hearing (Kral and Eggermont, 2007). Atrophy in deep layers of the auditory cortex disrupts long-range connections, restricting communication with higher-order auditory areas and thereby interfering with top-down processing and auditory object formation (Berger et al., 2017; Kral et al., 2017). Without significant input, association areas of the auditory system show increased weighting of inputs from the visual and somatosensory cortices (Meredith and Lomber, 2011). Electrophysiological studies have shown that early access to sound with cochlear implants can mitigate some of these effects in animal models (Review: Kral and Eggermont, 2007) and promote cortical development in children who receive cochlear implants (Jiwani et al., 2016). However, cochlear implants do not provide normal access to sound (Wilson, 2008) and thus are unlikely to completely restore the normal auditory connectome even in children who receive implants in both ears at young ages. Differences in the mechanisms supporting hearing in bilateral cochlear implant users may be revealed by investigating functional cortical interactions during listening.

1.3. Functional connectivity measured by EEG

Dynamic connections between specialized cortical areas are mediated through synchronous activity and give rise to higher-order perceptual and cognitive functions (Fries, 2005). Disruptions in these connections can lead to functional deficits as shown, for example, by a correlation between increased average path length and lower scores on a test of cognitive function in Alzheimer's disease (Stam et al., 2007). Evoked EEGs are commonly used to assess auditory development (e.g. Polonenko et al., 2017) and cross-modal plasticity (e.g. Doucet et al., 2006). The present study represents one of the few to assess connectivity within the cochlear implant population using EEG. Maglione et al. (2017) used theta and alpha connectivity to differentiate performance across different implant processors and several other groups have used imaging modalities such as functional near-infrared spectroscopy (fNIRS) (McKay et al., 2016; Anderson et al., 2017; Chen et al., 2017) and positron emission tomography (PET) (Wong et al., 1999) to assess cortical auditory networks in adults with CIs. EEG connectivity has largely been studied in the context of populations with neurological diseases such as Alzheimer's disease (Stam et al., 2007). Using EEG, independent networks can be resolved at different frequencies reflecting distinct neural processes. Gilley et al. (2014) related abnormal neural coupling in the alpha (8–13 Hz) and beta (13–30 Hz) ranges to behavioural test outcomes in children with language-learning problems.

Cortical evoked potentials are derived predominantly from oscillatory components in the theta (5–8 Hz) and alpha (8–13 Hz) ranges (Klimesch et al., 2004). Theta range coherence is a fundamental component of long-range neural communication (Başar et al., 2001) and is impacted by sensory and cognitive loading (Güntekin and Yener, 2008). Anderson et al. (2010) showed that the medial temporal lobe drives the prefrontal cortex using theta-band oscillations in memory processing. Coherence in the alpha band has also been shown to be affected by sensory processing (Schürmann and Başar, 2000) as well as attention modulation (Mazaheri et al., 2014). One major hypothesis is that alpha plays an inhibitory role, helping to suppress unimportant stimuli (Foxe and Snyder, 2011). On the other hand, Palva and Palva (2007) argue that synchronized alpha oscillations play a direct role in cortical processes involving memory and sensory awareness.

Multi-channel EEG provides a method to capture neural activity which can be used to construct functional network models of cortical processes. This is done by computing a metric of coupling between different channels or estimated sources, which are assumed to originate from different cortical locations, and building a model of resulting pairwise connections. Source reconstruction offers several advantages for quantifying EEG connectivity, including increasing spatial resolution (Michel et al., 2004) and reducing the effect of volume conduction. Finally, parcellation based on an anatomical atlas facilitates the interpretation of results by giving them context. It was shown in Lehmann et al. (2006) that networks calculated at the scalp level had minimal correspondence to a model using LORETA source estimates, however more work is needed in this area. It is possible to investigate these networks in either task-based or resting-state paradigms. While speech stimuli are commonly used to assess language networks, the use of non-meaningful transient stimuli provides an opportunity to assess fundamental cortical mechanisms involved with auditory processing. For example, cortical responses to simple pulsatile cochlear implant stimulation have effectively demonstrated abnormalities in bilateral auditory development in animals models of asymmetric hearing loss (Tillein et al., 2016) as well as in children with asymmetric hearing loss (Polonenko et al., 2017).

Methods from graph theory have been successfully applied to functional imaging data to quantify cortical networks (Review: Rubinov and Sporns, 2010). Coherence is a straightforward frequency-domain measure of correlation which can be applied between different cortical areas, analogous to the use of Pearson's correlation coefficient in fMRI studies (van den Heuvel and Hulshoff Pol, 2010). On the other hand, common volume conducted components in signals can be mistaken for independent sources with strong connectivity. Volume conduction can be mitigated both by beamforming and by looking at a change in coherence from baseline. The former accounts for the conductivity of a template head model which aims to undo the superposition of volume conducted sources in order to provide spatial specificity and the latter, baseline correction, removes effects of volume conduction that are fixed across time and source strength (Schoffelen and Gross, 2009). Imaginary coherence also provides a solution. By ignoring the real-part which has no phase lag, imaginary coherence is insensitive to spurious connections caused by volume conduction (Nolte et al., 2004), which plays a significant role in EEG data. Imaginary coherence has already been successfully applied in an EEG study of autism (García Domínguez et al., 2013). It should be noted that imaginary coherence systematically underestimates connectivity due to the non-uniqueness of phase and is biased by the absolute phase of the coherence (Stam et al., 2007).

In the present study, we calculated imaginary coherence between cortical source responses to sound to determine functional connectivity measures of EEG in children. We hypothesized that, in children: 1) bilateral hearing normally involves an increase in interhemispheric auditory connectivity; 2) connectivity between left and right auditory cortices is disrupted in children who are profoundly deaf and use bilateral cochlear implants; and 3) bilateral cochlear implants do not eliminate deafness-related development reorganization.

2. Methods and materials

2.1. Data collection

Cortical responses were collected in 16 children (4 girls) with prelingual deafness who received bilateral cochlear implants (CIs) in the same surgery (simultaneously) at 2.0 ± 0.9 years of age. Testing occurred when they were 6.0 ± 0.7 years of age and had 4.0 ± 1.0 years of bilateral CI experience. Responses were compared to those evoked in a control group of 13 typically developing children with normal hearing (6 girls) aged 5.1 ± 1.0 years. The groups were matched based on duration of hearing experience; therefore, the CI users were chronologically older than the control group at the time of testing. The study was approved by the Hospital for Sick Children's Research Ethics board, (Study

#1000002954), and written consent was obtained prior to data collection. Initial analyses focused on peak dipoles in auditory cortices and were published (Easwar et al., 2017). The data were further assessed in the present study for functional connectivity between cortical sources as indexed by the strength of both the magnitude and the imaginary part of coherence.

2.2. Electrophysiological recording

The SynAmps2 64-channel EEG system was used to record cortical auditory evoked potentials in both cohorts. Stimuli were 100 μs click-stimuli through ER-3A insert earphones in children with normal hearing or biphasic electrical pulses (25 μs/phase) delivered by apical electrodes (#20) in children with CIs. Both stimuli were presented in 36 ms, 250 Hz pulse trains with an inter-stimulus interval of 1 Hz. Stimuli were presented in three conditions in each child: unilateral left, unilateral right, and bilateral stimulation. Current levels were determined in CI users by recording auditory brainstem responses (ABRs) and matching wave eV amplitudes (Gordon et al., 2016). In children with normal hearing, stimuli were delivered at 50 dB over hearing threshold to the same stimuli. The EEG data were collected with a right earlobe reference at a sampling rate of 1 kHz and bandpass filtered from 0.15 Hz to 100 Hz. Trials were rejected if the amplitude at Cz was greater than 100 μV, if the amplitude at FPz was greater than 90 μV to account for eye-blinks, or if a global variance criterion of 1.0 nV^2 was exceeded. The data were re-referenced to the scalp average after rejecting noisy trials and channels. Data analysis was performed in MATLAB R2017b using the FieldTrip toolbox (Oostenveld et al., 2011) and custom scripts which are available upon request.

2.3. Source reconstruction

Source activity in each voxel within the brain was estimated using the Time-Restriction and Artifact and Coherent Source Suppression (TRACS) beamformer (Wong and Gordon, 2009) implemented to work with the FieldTrip toolbox. This beamformer is a variant of the linearly constrained minimum variance (LCMV) beamformer that accounts for cochlear implant artifacts and provides region suppression to prevent beamformer failure due to coherent activity in the left and right auditory cortices. An age-appropriate 3-layer boundary-element head model was created previously using the template-o-matic toolbox (Wilke et al., 2008) and used along with the electrode positions to calculate the lead field on a regular 3 mm isotropic grid. The beamformer then computed a set of optimized weights based on the lead-field matrix and an estimate of the individual data covariance. In contrast to previous studies using the TRACS beamformer which used a restricted window to estimate the covariance of the responses, the entire post-artifact time window was used in this study. A window of −80 to 15 ms was used to define the cochlear implant artifact (Wong and Gordon, 2009). Multiplying these weights with the scalp-level average-referenced EEG data yielded estimated virtual channels at each point in the source space. After normalizing by the estimated noise (Vrba and Robinson, 2001), Pseudo-Z time series were obtained for each of the virtual channels. The virtual channels were then interpolated onto the Automated-Anatomical Labelling atlas (AAL) (Tzourio-Mazoyer et al., 2002). Disregarding the cerebellar regions, this atlas defines 90 cortical regions, each of which contains many voxels of the original distributed source space. The voxel – and its corresponding virtual channel - with the highest signal-to-noise ratio (SNR) within each atlas region during the response window of 50–200 ms was chosen to represent the entire region (Drakesmith et al., 2015). This dramatic reduction in the number of virtual channels made it computationally feasible to look at coherence between every pair of sources.

2.4. Connectivity analysis

In order to calculate functional connectivity between the 90 cortical regions, the source response in each virtual channel was transformed into its time-frequency representation using the convolution method implemented in FieldTrip (Oostenveld et al., 2011). The frequency-dependent window size was chosen to be equal to two periods and the step size was 20 ms. Subsequently, coherence was calculated pairwise across all of the atlas regions and the result was baseline-corrected. Coherence is complex-valued and can thus be decomposed into real and imaginary components. In this study, both the imaginary part and magnitude were taken as metrics of inter-areal functional connectivity. This produced a 2D representation for each metric in the time-frequency plane for each of the 4005 unique connections. For analyses of interhemispheric connectivity, connectivity between the 6 temporal parcels in each hemisphere was averaged.

To construct network graphs for each subject, edge weights were defined by their coherence in the theta band (5–8 Hz). Next, peak connectivity was found within the 100–200 ms window, corresponding approximately to the full-width half max of the theta power in the group average spectrograms (not shown). The edge weights are represented in a 90 x 90 adjacency matrix that is symmetric because its connections are undirected; the metric measures associations between nodes rather than any causal influence of one over another. Group average networks were constructed by averaging the z-scored adjacency matrices across subjects. EEG data from an example participant shown in Fig. 1 outline key analysis steps: evoked potentials, source activity recovered using the beamformer, atlas parcellation, time-frequency decomposition, and the resulting model of network connectivity in the theta range.

2.5. Statistical analysis on cortical networks

Statistical analysis on network models was performed using the Network-Based Statistics toolbox which allowed for group hypothesis testing while controlling a family-wise error rate of 0.05% (Zalesky et al., 2010). The NBS toolbox proceeds in two major steps to perform statistical tests on connectivity data. First, univariate hypothesis testing is performed across all connections included within a chosen threshold to identify a network to test for significance. Next, a set of 5000 networks were generated by permuting the connections in the underlying matrices between groups. A significant network (a set of nodes and their connections) is found when its extent (size) exceeds the null distribution. The framework does not guarantee the statistical significance of individual connections; however, it provides an increase in sensitivity over connection-wise statistical tests for connected networks.

3. Results

3.1. Early auditory processing is supported by interhemispheric connections

Robust evoked responses were elicited in both groups and all stimulus conditions. After source localization, connectivity was measured by imaginary coherence across 4005 connections (pairwise between 90 atlas regions) in each group and stimulus condition. Global connectivity, the average across all 4005 connections, is shown in Fig. 2. A peak in both theta and alpha connectivity can be seen between 100 and 200 ms in all conditions. The normal hearing group showed an increase in theta-band coherence when stimulated bilaterally relative to unilaterally.

Accordingly, theta-band coherence maps were generated within the same time window of 100–200 ms. Fig. 3 shows networks comprising the top 8 (0.2% of the total 4005 possible) most coherent connections in both groups for all three stimulus conditions. Most consistent across all six mean networks (3 stimulus conditions x 2 groups) were the many interhemispheric connections between temporal cortices. Networks evoked by unilateral stimulation in children with normal hearing involved contralateral frontal areas whereas these connections were not found in children with bilateral CIs.

A mixed two-way repeated measures ANOVA of all 4005 possible connections with group and ear of stimulation as factors was performed

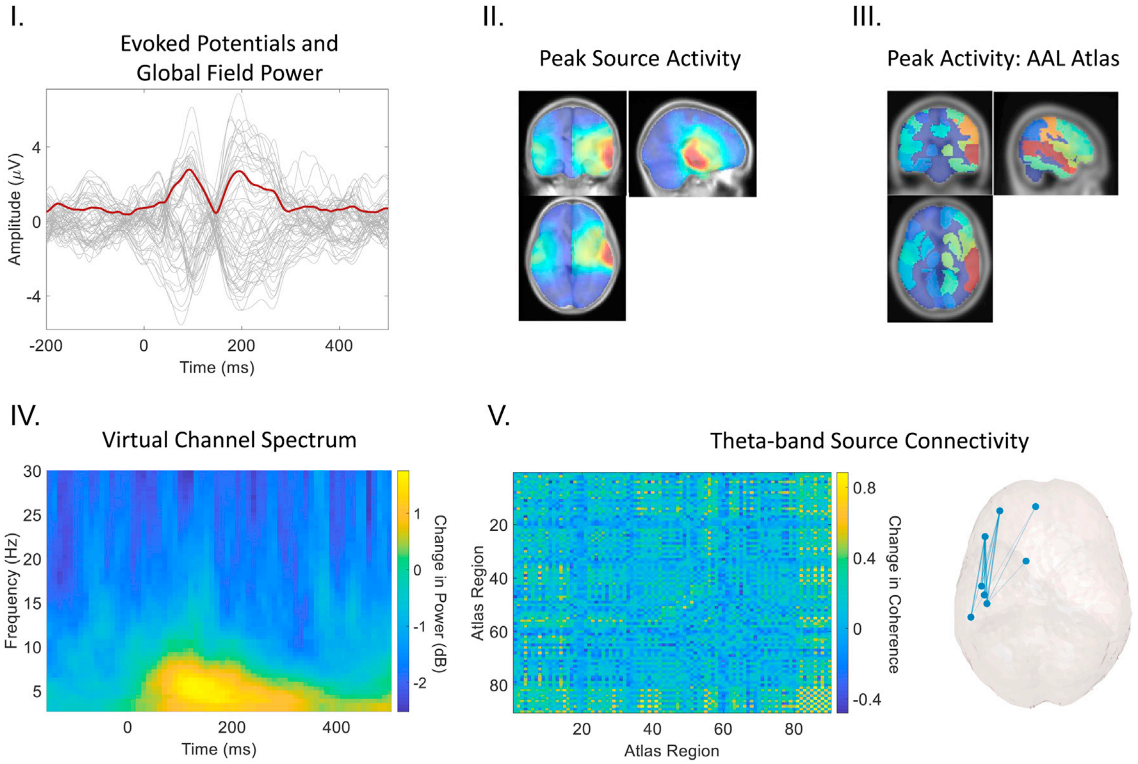

Fig. 1. Procedure for measuring cortical connectivity from EEG signals. I) Global field power of recorded EEG data (shown in red) **is** used to define the time window of evoked activity. II) The TRACS beamformer then provides source-space estimates of the EEG responses that can be combined with MRI images to estimate simulated functional activation at each voxel. III) Voxel-based peak activations are interpolated onto the AAL atlas. IV) Source time series from each of the 90 areas in the AAL atlas are then transformed into their time-frequency representation. V) Metrics of connectivity, such as imaginary coherence, produce an adjacency matrix of connections between network nodes. By applying a threshold, the resulting graph can be visualized in a 3D model. Brain images are presented such that the left hemisphere appears on the left side of the image.

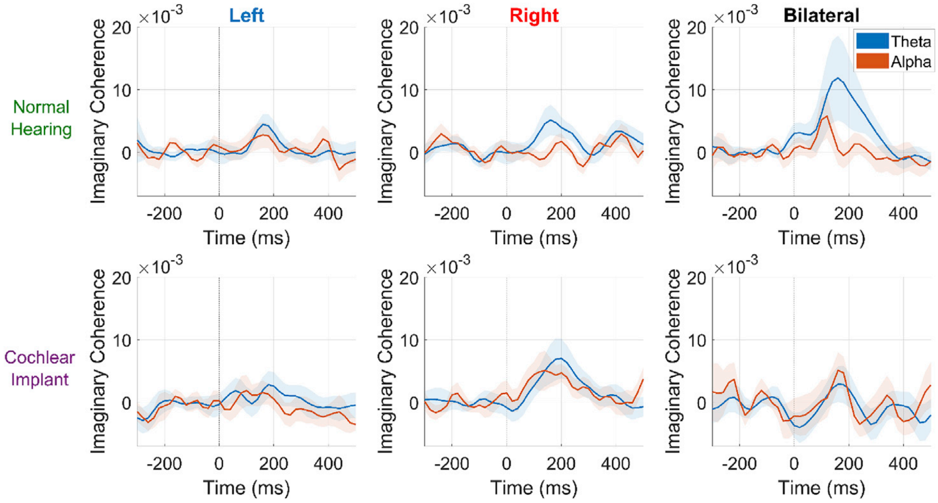

Fig. 2. Global connectivity as measured by the average imaginary coherence across 4005 connections (unique pairs between 90 virtual channels) shows that the cortical networks supporting passive listening exhibits peak connectivity between 100 and 200 ms post stimulus in all groups and stimulus conditions. The shaded areas denote ±1 standard error of the mean.

using the network-based statistic. Although no significant overall group differences were identified ($F(1, 27) = 7$, $p = 1.0$) owing to very few super-threshold edges compared to the null distribution, there were two significant group by stimulus interaction networks ($F(2, 27) = 6$, $p = 0.018$) and ($F(2, 27) = 6$, $p < 0.001$) (networks not shown), suggesting that the effect of stimulus differs between groups. Independent analyses indicated significant group contrast networks in bilateral and left stimulus (one-tailed post-hoc t-tests accounting for multiple comparisons; false discovery rate $= q < 0.05$). There were no significant group network differences in the right stimulus condition but further investigation of each connection under right stimulation (corrected with a false discovery rate $= q < 0.025$) revealed a single significant connection between the right angular gyrus and right frontal lobe that was stronger in the CI cohort.

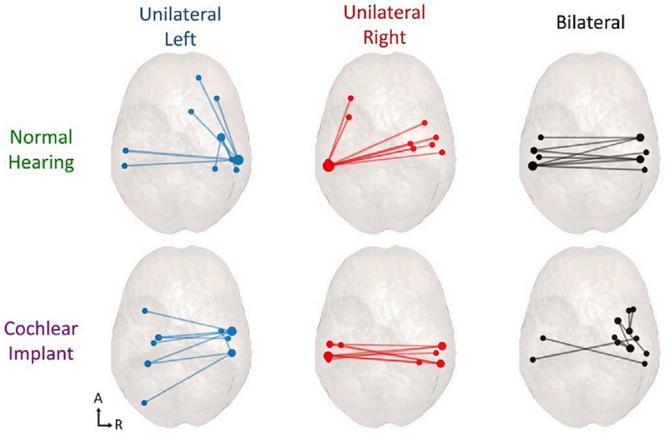

Fig. 3. Graph plots in cortical source space show the top connections from a group-average of the z-scored magnitude of theta-band coherence for visualization purposes. Results are shown for unilateral left, unilateral right, and bilateral stimulus presentation in both groups of children. The connections predominantly connect the bilateral temporal areas. The nodes are located at the centroids of the AAL regions that they represent. Node size is weighted by the degree of each connection. Connections may reflect any combination of underlying causal interactions between the temporal cortices or that bottom-up auditory input drove these regions in similar ways, independently. These connections between the auditory regions confirm the coordinated involvement of both auditory cortices in processing both unilaterally and bilaterally presented sound. Brain images are presented as cranial-caudal projections; the left hemisphere appears on the left side of the image.

3.2. Bilateral connectivity between auditory cortices is reduced in children using CIs

Imaginary coherence between temporal cortices was assessed for each condition in both groups. The time courses of these measures in theta and alpha bands are shown in Fig. 4A. Peaks between 100 and 200 ms are evident in each condition (most prevalent in the theta band), reflecting connectivity underlying the early latency component of the auditory response. While alpha coherence between the temporal cortices appears to parallel theta coherence, 2-way mixed-effects ANOVA revealed no significant differences between groups ($F(1,27) = 0.17$, $p = 0.68$), nor group × stimulus interactions ($F(2,27) = 2.8$, $p = 0.068$). Furthermore, attention was not measured during this passive listening experiment, so the remaining analyses focus on coherence in the theta band.

Peak coherence in the 100–200 ms time window is plotted by stimulus condition in each group in Fig. 4B. As shown, peak imaginary coherence was reduced in the children with CIs but only in the bilateral condition (2-way mixed-effects ANOVA: group * stimulus: $F(2, 27) = 3.69$, $p = 0.03$; Post-hoc Wilcoxon rank-sum test, $p < 0.05$). The difference in imaginary coherence between the bilateral and averaged unilateral condition in each group are shown in Fig. 4C. Increased imaginary coherence, representing binaural facilitation was found in children with normal hearing but decreased coherence was found in the bilateral CI group. Significant differences in binaural facilitation of connectivity between normal hearing and implant users were identified at 0–100 ms and 260–280 ms (Wilcoxon rank-sum test at each time point, $p = 0.05$, FDR corrected using the Benjamini-Hochberg Procedure (Thissen et al., 2016)).

3.3. Reorganization of connectivity in childhood deafness

Differences between groups in the bilateral stimulus condition were further explored across all 4005 possible connections. Two significant networks emerged from these analyses as shown in Fig. 5. The first network reflects significantly stronger connections in the normal hearing group than in cochlear implant users ($p < 0.002$) between central regions and the left temporal lobe. The second network consisted of connections between the occipital and frontal lobes that were significantly stronger in the cochlear implant group ($p = 0.01$).

4. Discussion

4.1. Audition is normally supported by connectivity between bilateral temporal cortices

In this study, electrophysiological responses were recorded from children with normal hearing and bilateral implants in response to transient auditory pulse/click trains. By calculating the connectivity between source-resolved anatomical areas, it was possible to determine which regions were synchronously engaged in response to auditory input. Averaged connectivity shown in Fig. 2 revealed peak coherence at early response latencies with less coherence thereafter. The timing of the coherence is in line with early obligatory cortical responses, reflecting auditory detection during passive listening with little higher order auditory processing. As shown in Fig. 3, the underlying networks responding at this early latency involved connections between the temporal areas mediated by theta coherence. This is consistent with the temporal generators known to underlie the cortical auditory evoked potential at similar latencies (Naatanen and Picton, 1987). In addition, white matter tracts of the corpus callosum and anterior commissure provide pathways for connectivity between the bilateral auditory cortices (Javad et al., 2014) and dense callosal fibers link the core and belt regions between bilateral auditory cortices (Kaas and Hackett, 2000). The callosal auditory fibers, in particular, have large axonal diameters to facilitate transmission between these timing-sensitive areas (Aboitiz and Montiel, 2003).

Coherence between the temporal areas of the brain in the present cohort of children with normal hearing demonstrated that the bilateral auditory cortices show greater synchronization during bilateral stimulation compared to unilateral conditions. We have considered the possibility that these increases reflect a change in SNR within the frequency band under study, which might have spuriously inflated the estimate of connectivity (Bastos and Schoffelen, 2015); however, this is unlikely to account for the change in only the group with normal hearing because the evoked responses recorded in both CI and normal hearing groups showed similar increases in SNR. Facilitation of connectivity in the bilateral compared to unilateral listening condition in children with normal hearing supports evidence of increased cortical processing within temporal and other cortical areas required to interpret binaural input for the purposes of spatial hearing (Salminen et al., 2012) and listening in noise (Lee et al., 2008). Increased coherence during bilateral stimulation could also reflect the high degree of correlation between inputs from each ear which provides increased redundancy and resilience for hearing one target auditory source in the presence of competing sounds (Semple and Kitzes, 1993).

4.2. Binaural integration is impaired in children using bilateral implants

In addition to communication, coherence between neural assemblies is important for integrating sensory inputs across modalities (Senkowski et al., 2008). Whereas theta-band coherence between the temporal cortices increased in the bilateral compared to unilateral conditions in children with normal hearing, this “binaural facilitation” was absent in children who use cochlear implants during at least two time windows during the response (0–100 ms and 260–280 ms, Fig. 4C). Given that children using cochlear implants show strong activation in both auditory cortices to unilateral stimulation (Polonenko et al., 2017; Easwar et al., 2017), these results suggest that peak responses in bilateral auditory areas of the brain lose the precise coordination measured in children with normal hearing. In support, both resting-state and task-based fNIRS studies have similarly reported decreased correlation between matching bilateral optodes over auditory areas in cochlear implant users relative to

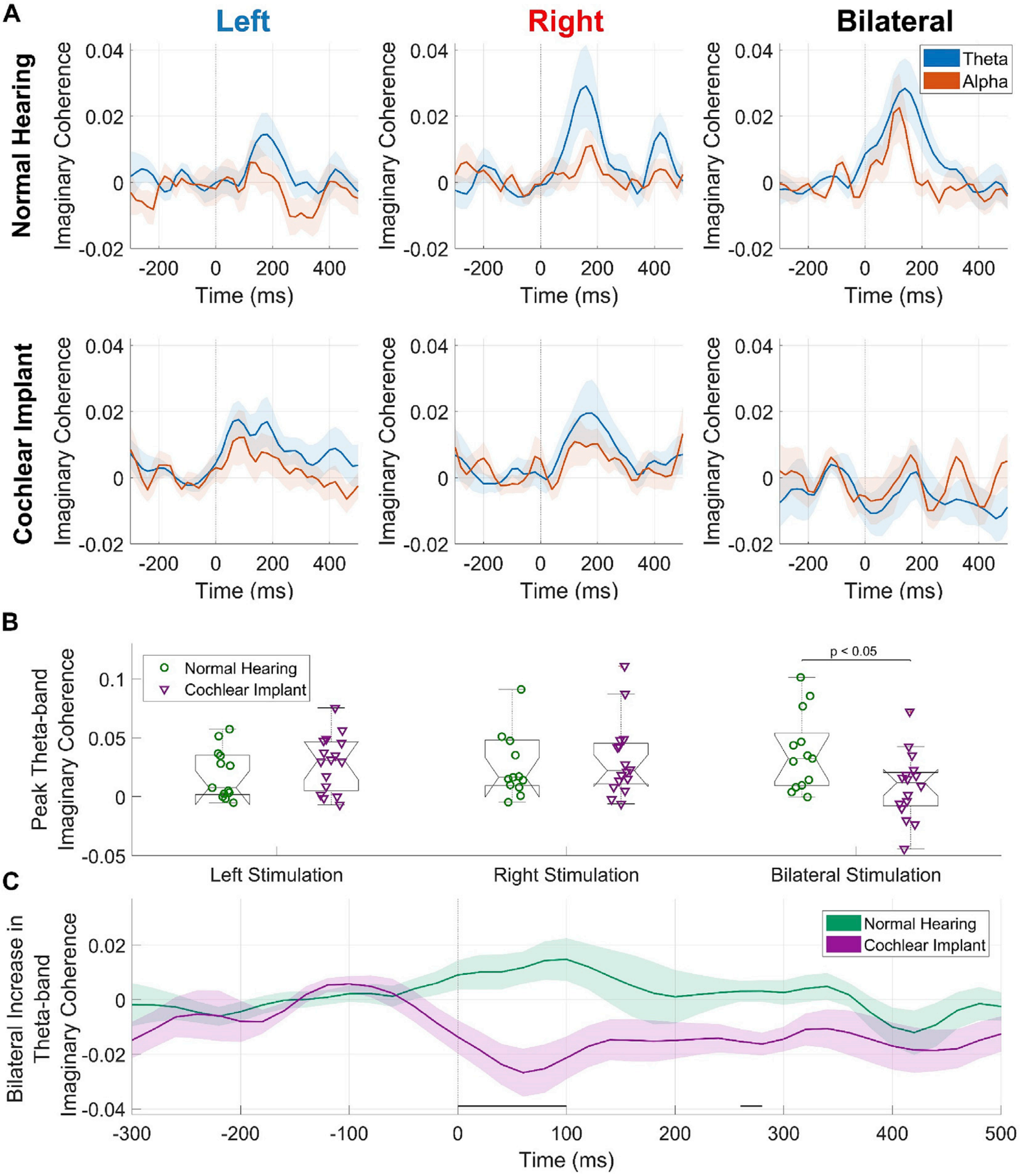

Fig. 4. A: Imaginary Coherence between the auditory cortices across time in each group and stimulus condition in the theta (5–8 Hz) and alpha (8–12 Hz) bands. B: The peak theta-band bilateral coherence in the bilateral condition is significantly different between the normal hearing and cochlear implant groups. C: Group average binaural facilitation of theta connectivity, which is the difference between bilateral and unilateral imaginary coherence, is significantly greater in normal hearing than CIs in the 0–100 ms and 260–280 ms windows post stimulus. The black bar denotes a significant difference ($p < 0.05$) in medians (Wilcoxon rank-sum, FDR-corrected in post-stimulus window.) The shaded areas represent ±1 standard error of the mean.

normal hearing (McKay et al., 2016; Chen et al., 2017). The findings of the present study provide the first evidence of decreased theta band coherence between the temporal cortices during bilateral cochlear implant stimulation in children at early stages of cortical processing (i.e. P1 responses of the electrically evoked cortical auditory evoked potential).

Poor coherence between bilateral auditory cortices in children using cochlear implants could reflect both the effects of deafness from early life as well as continued impairments in binaural hearing despite using cochlear implants in both ears.

Early onset deafness results in extensive changes throughout the auditory pathways, including changes to the nuclei and dystrophy in deep cortical layers (Butler and Lomber, 2013). While the rudimentary afferent pathways are hard-coded, auditory experience is necessary for further developing the auditory system's timing and microcircuitry (Kral and Sharma, 2013). Hearing in children begins prenatally but continues to mature in the first few years of life (Moore and Linthicum Jr, 2007). Deafness in early life disrupts auditory development and leads to reorganization of deprived pathways. The immature auditory brainstem cannot develop until significant input is provided (Gordon et al., 2013; Gordon et al., 2006; Gordon et al., 2007) and may reorganize during the period of deprivation as shown by morphological changes to the endbulb of held in deaf white cats (Baker et al., 2010) and abnormally reduced eN1-eII latencies in children who are deaf (Gordon et al., 2016). In the cortex, synaptogenesis and pruning are delayed in deaf white cats (Kral et al., 2017) and development is delayed and/or altered in children who are deaf (Kral and Sharma, 2013; Gordon and Kral, 2019). Moreover, evidence of corticocortical decoupling (Kral et al., 2017) and deterioration of binaural responses in cortical neurons (Tillein et al., 2016) in congenitally deaf white cats suggest deafness in early development

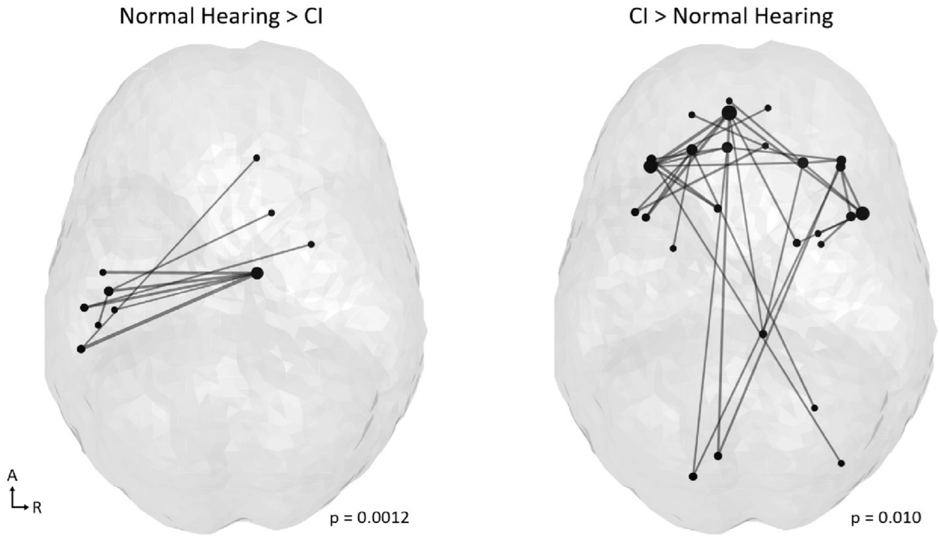

Fig. 5. Significant contrast networks from the bilateral condition between the normal hearing and implanted groups using the network-based statistic. The networks were significant over a range of t-thresholds, but the networks plotted were generated using T = 4 for Normal Hearing > CI and T = 3 for CI > Normal Hearing. Brain images are presented as cranial-caudal projections; the left hemisphere appears on the left side of the image.

compromises binaural processing. Early treatment of deafness aims to limit these changes within early sensitive developmental periods (Kral and O'Donoghue, 2010; Gordon et al., 2015). Indeed, children who receive cochlear implants in infancy (<9 months) show better outcomes than their peers implanted as toddlers (>1 years) (Ching recent data, available at https://www.outcomes.nal.gov.au/key-findings). Importantly, the children in the present study were provided with bilateral implants within this sensitive period.

The present findings of depressed integration of bilateral input in children using cochlear implants is consistent with their poor perception of interaural timing cues (Gordon et al., 2014) and spatial hearing measured by sound localization (Litovsky et al., 2006; Van Hoesel et al., 2010). Bilateral implants do help children detect speech in noise, particularly when separated in space (Chadha et al., 2011), but these spatial benefits remain impaired relative to children with normal hearing (Misurelli and Litovsky, 2015). These behavioural results can be explained, in part, by the crude temporal fine structure of CI stimulation which limits access to interaural timing cues and by distortions in interaural level and timing provided by the two independent speech processors. Furthermore, place mismatch between electrode arrays may disrupt coincidence of inputs in the brainstem (Gordon et al., 2012; Polonenko et al., 2018) and impair perceptual fusion (Kan et al., 2013; Steel et al., 2015). Together these problems hinder the process of tuning the pathways for binaural processing and prevent binaural integration.

It is possible that impaired coincidence of bilateral input in the auditory system, along with residual effects of early onset deafness, compromise the ability of the auditory system to integrate binaural input, thus impairing functional connectivity between the auditory cortices in response to bilateral input as measured in the present study.

4.3. Children with bilateral CIs recruit different cortical networks

The significant contrasts in the bilateral condition, shown in Fig. 5, reveal distinct networks in children with cochlear implants relative to their normally hearing peers. The network recruited preferentially in CI listeners, in Fig. 5, involved connections between the frontal and occipital lobes, suggesting increased visual processing during auditory stimulation. This could be attributed to residual effects of cross-modal reorganization (Lee et al., 2001; Stropahl et al., 2017) and/or an adaptive strategy that leverages visual processing to support listening (Lomber et al., 2010; Barone et al., 2016). Chen et al. (2017) also showed increased functional connectivity between the auditory and visual systems in individuals who receive cochlear implants in adulthood.

In addition to visual involvement, there have been reports of modulated connectivity between the auditory system and networks that are not modality specific in deaf individuals. Prefrontal areas are involved in a wide array of auditory processing tasks ranging from detection to language processing and receive projections from both lower and higher-order auditory areas (Plakke and Romanski, 2014). Furthermore, using positron-emission tomography, Giraud and Lee (2014) demonstrated that activation of a prefrontal network implicated in higher-order attentional and working memory processes was predictive of better speech perception in bilateral implant users. Using resting-state fMRI, Ding et al. (2016) reported that the salience network, involving the lateral frontal nodes proximal to the dorsal anterior cingulate cortex and the anterior insula, had increased connectivity with the superior temporal gyrus in CI users. While the authors focused on the benefit this provided for working memory, these changes may more broadly serve to compensate for auditory deficits by directing attention where needed.

The cohort of children using cochlear implants also showed deficits in a focused network involving interhemispheric connections between the left temporal cortex and right cingulate cortex (Fig. 5). Connections between the posterior cingulate cortex and the superior temporal gyrus have been discovered using PET imaging (Naito et al., 2000), although their function is not clear. The posterior cingulate cortex is a core component of the default mode network and may play a role in directing attention. It is known to be active when the brain is not actively engaged (Leech and Sharp, 2014). Thus, this finding may reflect increased attention to the ongoing auditory stimuli in children with CIs during passive listening, suggesting reduced ability to ignore the input relative to normal hearing peers.

Overall, results of the present study suggest that children with cochlear implants require increased use of a visually based network for hearing, more attention, and reduced use of a network involved in higher order auditory processing. This means that the basic structural and functional networks of their auditory system are subject to adaptation through reweighting of specific connections (Striem-Amit et al., 2016).

4.4. Summary and conclusion

In children with normal hearing, binaural hearing is supported by an increase in coherence at early latencies between bilateral auditory areas relative to unilateral hearing. The absence of this binaural facilitation in children with cochlear implants supports existing evidence of impaired binaural processing. A whole-brain coherence analysis revealed that cochlear implant users recruit a network that involves frontal and occipital regions, suggesting that some extra-temporal areas may remain involved during passive listening. Ultimately, these findings are consistent with developmental adaptation in children who are deaf and use cochlear implants to hear.

Credit author statement

Daniel Smieja: Methodology, Formal analysis, Software, Writing – Original Draft, Writing – Review & Editing. Benjamin T. Dunkley: Supervision, Writing – Review & Editing. Blake C. Papsin: Resources, Funding acquisition, Writing – Review & Editing. Vijayalakshmi Easwar: Investigation, Writing – Review & Editing. Hiroshi Yamazaki: Investigation, Writing – Review & Editing. Michael Deighton: Investigation. Karen A. Gordon: Conceptualization, Validation, Resources, Writing – Original Draft, Writing – Review & Editing, Project administration, Supervision, Funding acquisition.

Declaration of competing interest

KG is employed by the Hospital for Sick Children where she holds the Cochlear Americas Chair in Auditory Development. She has received travel support for conference attendance from Cochlear Corp, and Advanced Bionics; has consulted for the Government of Canada, Coast-Guard, and been a lecturer at Salus University.

BP is Otolaryngologist-in-Chief at The Hospital for Sick Children where he holds the Jordan and Lisa Gnat Family and Bastable-Potts Chair in Otolaryngology. He has received travel support for conference attendance from Cochlear Corp. and been a lecturer at Salus University.

DS, BD, VE, MD, and HY declare no competing interests.

Acknowledgements

This work was supported by a Restracomp award (to D.S.) and the Canadian Institutes of Health Research (MOP-97924 to KG). The authors would like to thank the participants and their families as well as the team at Archie's cochlear implant laboratory.

References

Aboitiz, F., Montiel, J., 2003. One hundred million years of interhemispheric communication: the history of the corpus callosum. Braz. J. Med. Biol. Res. 36, 409–420.

Anderson, C.A., Lazard, D.S., Hartley, D.E.H., 2017. Plasticity in bilateral superior temporal cortex: effects of deafness and cochlear implantation on auditory and visual speech processing. Hear. Res. 343, 138–149.

Anderson, K.L., Rajagovindan, R., Ghacibeh, G.A., Meador, K.J., Ding, M., 2010. Theta oscillations mediate interaction between prefrontal cortex and medial temporal lobe in human memory. Cerebr. Cortex 20, 1604–1612.

Baker, C.A., Montey, K.L., Pongstaporn, T., Ryugo, D.K., Cant, N.B., 2010. Postnatal development of the endbulb of Held in congenitally deaf cats. Front. Neuroanat. 4, 1–14.

Barone, P., Chambaudie, L., Strelnikov, K., Fraysse, B., Marx, M., Belin, P., et al., 2016. Crossmodal interactions during non-linguistic auditory processing in cochlear-implanted deaf patients. Cortex 83, 259–270.

Başar, E., Başar-Eroglu, C., Karakaş, S., Schurmann, M., 2001. Gamma , alpha , delta , and theta oscillations govern cognitive processes. Int. J. Psychophysiol. 241–248.

Bastos, A.M., Schoffelen, J.-M., 2015. A tutorial review of functional connectivity analysis methods and their interpretational pitfalls. Front. Syst. Neurosci. 9, 175.

Berger, C., Kühne, D., Scheper, V., Kral, A., 2017. Congenital deafness affects deep layers in primary and secondary auditory cortex. J. Comp. Neurol. 525, 3110–3125.

Butler, B.E., Lomber, S.G., 2013. Functional and structural changes throughout the auditory system following congenital and early-onset deafness: implications for hearing restoration. Front. Syst. Neurosci. 7, 1–17.

Chadha, N.K., Papsin, B.C., Jiwani, S., Gordon, K.A., 2011. Speech detection in noise and spatial unmasking in children with simultaneous versus sequential bilateral cochlear implants. Otol. Neurotol. 32, 1057–1064.

Chen, L.C., Puschmann, S., Debener, S., 2017. Increased cross-modal functional connectivity in cochlear implant users. Sci. Rep. 7, 1–10.

Cullington, H.E., Bele, D., Brinton, J.C., Cooper, S., Daft, M., Harding, J., et al., 2017. United Kingdom national paediatric bilateral project: results of professional rating scales and parent questionnaires. Cochlear Implants Int. 18, 23–35.

Ding, H., Ming, D., Wan, B., Li, Q., Qin, W., Yu, C., 2016. Enhanced spontaneous functional connectivity of the superior temporal gyrus in early deafness. Sci. Rep. 6, 1–11.

Doucet, M.E., Bergeron, F., Lassonde, M., Ferron, P., Lepore, F., 2006. Cross-modal reorganization and speech perception in cochlear implant users. Brain 3376–3383.

Drakesmith, M., Dimitriadis, S., Brindley, L., Jones, D.K., Singh, K., Linden, D., et al., 2015. Information Theoretic Evaluation of Methods for Constructing Functional Connectomes from MEG.

Easwar, V., Yamazaki, H., Deighton, M., Papsin, B., Gordon, K., 2017. Simultaneous bilateral cochlear implants : developmental advances do not yet achieve normal cortical processing. Brain Behav. 1–15.

Foxe, J.J., Snyder, A.C., 2011. The role of alpha-band brain oscillations as a sensory suppression mechanism during selective attention. Front. Psychol. 2, 154.

Fries, P., 2005. A mechanism for cognitive dynamics : neuronal communication through neuronal coherence. Trends Cogn. Sci. 9.

García Domínguez, L., Stieben, J., Pérez Velázquez, J.L., Shanker, S., 2013. The imaginary part of coherency in autism: differences in cortical functional connectivity in preschool children. PLoS One 8.

Gilley, P.M., Walker, N.K., 2014. Abnormal oscillatory neural coupling in children with language-learning problems and auditory processing disorder. Semin. Hear. 1, 15–26.

Giraud, A., Lee, H., 2014. Predicting cochlear implant outcome from brain organisation in the deaf. Restor. Neurol. Neurosci. 25, 381–390.

Gordon, K., Kral, A., 2019. Animal and human studies on developmental monaural hearing loss. Hear. Res. 380, 60–74.

Gordon, K.A., Papsin, B.C., Harrison, R.V., 2006. An evoked potential study of the developmental time course of the auditory nerve and brainstem in children using cochlear implants. Audiol. Neurotol. 11, 7–23.

Gordon, K.a., Salloum, C., Toor, G.S., van Hoesel, R., Papsin, B.C., 2012. Binaural interactions develop in the auditory brainstem of children who are deaf: effects of place and level of bilateral electrical stimulation. J. Neurosci. 32, 4212–4223.

Gordon, K., Henkin, Y., Kral, A., 2015. Asymmetric hearing during development: the aural preference syndrome and treatment options. Pediatrics 136, 141–153.

Gordon, K.A., Abbasalipour, P., Papsin, B.C., 2016. Balancing current levels in children with bilateral cochlear implants using electrophysiological and behavioral measures. Hear. Res. 335, 193–206.

Gordon, K.A., Deighton, M.R., Abbasalipour, P., Papsin, B.C., Ptito, M., 2014. Perception of binaural cues develops in children who are deaf through bilateral cochlear implantation. PLoS One 9, 1–25.

Gordon, K.A., Valero, J., Papsin, B.C., 2007. Binaural processing in children using bilateral cochlear implants. Neuroreport 18 (6), 613–617.

Gordon, K.A., Wong, D.D.E., Papsin, B.C., 2013. Bilateral input protects the cortex from unilaterally-driven reorganization in children who are deaf. Brain 136, 1609–1625.

Güntekin, B., Yener, G., 2008. Decrease of evoked delta , theta and alpha coherences in Alzheimer patients during a visual oddball paradigm. Brain Res. 5.

Hawley, M.L., Litovsky, R.Y., Culling, J.F., 2004. The benefit of binaural hearing in a cocktail party: effect of location and type of interferer. J. Acoust. Soc. Am. 115, 833–843.

van den Heuvel, M.P., Hulshoff Pol, H.E., 2010. Exploring the brain network: a review on resting-state fMRI functional connectivity. Eur. Neuropsychopharmacol. 20, 519–534.

Van Hoesel, R.J.M., Tyler, R.S., Tyler, R.S., 2010. Speech perception , localization , and lateralization with bilateral cochlear implants Speech perception , localization , and lateralization with bilateral cochlear implants. J. Acoust. Soc. Am. 1617.

Javad, F., Warren, J.D., Micallef, C., Thornton, J.S., Golay, X., Yousry, T., et al., 2014. Auditory tracts identified with combined fMRI and diffusion tractography. Neuroimage 84, 562–574.

Jiwani, S., Papsin, B.C., Gordon, K.A., 2016. Early unilateral cochlear implantation promotes mature cortical asymmetries in adolescents who are deaf. Hum. Brain Mapp. 37, 135–152.

Kaas, J.H., Hackett, T.A., 2000. Subdivisions of auditory cortex and processing streams in primates. Proc. Natl. Acad. Sci. 97, 11793–11799.

Kan, A., Stoelb, C., Litovsky, R.Y., Goupell, M.J., 2013. Effect of mismatched place-of-stimulation on binaural fusion and lateralization in bilateral cochlear-implant users a). J. Acoust. Soc. Am. 53705, 2923–2936.

Klimesch, W., Schack, B., Schabus, M., Doppelmayr, M., Gruber, W., Sauseng, P., 2004. Phase-locked alpha and theta oscillations generate the P1–N1 complex and are related to memory performance. Cogn. Brain Res. 302–316.

Kral, A., Eggermont, J.J., 2007. What's to lose and what's to learn: development under auditory deprivation, cochlear implants and limits of cortical plasticity. Brain Res. Rev. 56, 259–269.

Kral, A., O'Donoghue, G.M., 2010. Profound deafness in childhood. N. Engl. J. Med. 15, 1438–1450.

Kral, A., Sharma, A., 2013. Developmental neuroplasticity after cochlear implantation. Trends Neurosci. 35, 111–122.

Kral, A., Yusuf, P.A., Land, R., 2017. Higher-order auditory areas in congenital deafness: top-down interactions and corticocortical decoupling. Hear. Res. 343, 50–63.

Lee, D.S., Lee, J.S., Oh, S.H., Kim, S.-K., Kim, J.-W., Chung, J.-K., et al., 2001. Cross-modal plasticity and cochlear implants. Nature 409, 149–150.

Lee, E.R., Wong, P.C., Dhar, S., Gunesekera, G.M., Abel, R.A., 2008. Cortical mechanisms of speech perception in noise in elderly listeners. J. Acoust. Soc. Am. 123, 3073–3073.

Leech, R., Sharp, D.J., 2014. The role of the posterior cingulate cortex in cognition and disease. Brain 12–32.

Lehmann, D., Faber, P.L., Gianotti, L.R.R., Kochi, K., Pascual-Marqui, R.D., 2006. Coherence and phase locking in the scalp EEG and between LORETA model sources, and microstates as putative mechanisms of brain temporo-spatial functional organization. J. Physiol. Paris 99, 29–36.

Litovsky, R., Johnstone, P., Godar, S., Agrawal, S., 2006. Bilateral cochlear implants in children: localization acuity measured with minimum audible angle [Internet]. Ear 2006Available from. http://www.ncbi.nlm.nih.gov/pmc/articles/PMC2651156/.

Litovsky, R.Y., Gordon, K., 2016. Bilateral cochlear implants in children: effects of auditory experience and deprivation on auditory perception. Hear. Res. 338, 76–87.

Lomber, S.G., Meredith, M.A., Kral, A., 2010. Cross-modal plasticity in specific auditory cortices underlies visual compensations in the deaf. Nat. Neurosci. 13, 1421–1427.

Maglione, A.G., Cartocci, G., Modica, E., Rossi, D., Colosimo, A., Di, G., et al., 2017. Evaluation of different cochlear implants in unilateral hearing patients during word listening tasks : a brain connectivity study *. IEEE 2470–2473.

Mazaheri, A., van Schouwenburg, M.R., Dimitrijevic, A., Denys, D., Cools, R., Jensen, O., 2014. Region-specific modulations in oscillatory alpha activity serve to facilitate processing in the visual and auditory modalities. Neuroimage 87, 356–362.

McKay, C.M., Shahm, A., Seghouane, A.-K., Zhou, X., Cross, W., Litovsky, R., 2016. Connectivity in language areas of the brain in cochlear implant users as revealed by fNIRS. Adv. Exp. Med. Biol. 894, 327–336.

Meredith, A.M., Lomber, S.G., 2011. Somatosensory and visual crossmodal plasticity in the anterior auditory field of early-deaf cats. Hear. Res. 280, 1–23.

Michel, C.M., Murray, M.M., Lantz, G., Gonzalez, S., Spinelli, L., Grave De Peralta, R., 2004. EEG source imaging. Clin. Neurophysiol. 115, 2195–2222.

Misurelli, S.M., Litovsky, R.Y., 2015. Spatial release from masking in children with bilateral cochlear implants and with normal hearing: effect of target-interferer similarity. J. Acoust. Soc. Am. 138, 319–331.

Moore, J.K., Linthicum Jr., F.H., 2007. The human auditory system : a timeline of development. Int. J. Audiol. 46, 460–478.

Naatanen, R., Picton, T.W., 1987. The N1 wave of the human electric and magnetic response to sounds: a review and a analysis of the component structure. Psychophysiology 24, 375–425.

Naito, Y., Tateya, I., Fujiki, N., Hirano, S., Ishizu, K., Nagahama, Y., et al., 2000. Increased cortical activation during hearing of speech in cochlear implant users. Hear. Res. 143, 139–146.

Nolte, G., Bai, O., Wheaton, L., Mari, Z., Vorbach, S., Hallett, M., 2004. Identifying true brain interaction from EEG data using the imaginary part of coherency. Clin. Neurophysiol. 115, 2292–2307.

Oostenveld R, Fries P, Maris E, Schoffelen JM. FieldTrip: open source software for advanced analysis of MEG, EEG, and invasive electrophysiological data. Comput. Intell. Neurosci. 2011; 2011.

Palva, S., Palva, J.M., 2007. New vistas for a -frequency band oscillations. Trends Neurosci. 30.

Plakke, B., Romanski, L.M., 2014. Auditory connections and functions of prefrontal cortex. Front. Neurosci. 8, 1–13.

Polonenko, M.J., Gordon, K.A., Cushing, S.L., Papsin, B.C., 2017. Cortical organization restored by cochlear implantation in young children with single sided deafness. Sci. Rep. 7, 1–8.

Polonenko, M.J., Papsin, B.C., Gordon, K.A., 2018. Limiting asymmetric hearing improves benefits of bilateral hearing in children using cochlear implants. Sci. Rep. 1–17.

Rubinov, M., Sporns, O., 2010. Complex network measures of brain connectivity: uses and interpretations. Neuroimage 52, 1059–1069.

Salminen, N.H., Tiitinen, H., May, P.J.C., 2012. Auditory spatial processing in the human cortex. The Neuroscientist 18, 602–612.

Schoffelen, J.M., Gross, J., 2009. Source connectivity analysis with MEG and EEG. Hum. Brain Mapp. 30, 1857–1865.

Schürmann, M., Başar, E., 2000. Functional aspects of alpha oscillations in the EEG. Int. J. Psychophysiol. 39, 151–158.

Semple, N., Kitzes, L.M., 1993. Focal selectivity for binaural sound pressure level in cat primary auditory Cortex : two-way intensity network tuning. J. Neurophysiol. 69.

Senkowski, D., Schneider, T.R., Foxe, J.J., Engel, A.K., 2008. Crossmodal binding through neural coherence: implications for multisensory processing. Trends Neurosci. 31, 401–409.

Sharma, A., Campbell, J., Cardon, G., 2015. Developmental and cross-modal plasticity in deafness: evidence from the P1 and N1 event related potentials in cochlear implanted children. Int. J. Psychophysiol. 95, 135–144.

Stam, C.J., Jones, B.F., Nolte, G., Breakspear, M., Scheltens, P., 2007. Small-world networks and functional connectivity in Alzheimer's disease. Cerebr. Cortex 17, 92–99.

Steel, M.M., Papsin, B.C., Gordon, K.A., 2015. Binaural fusion and listening effort in children who use bilateral cochlear Implants : a psychoacoustic and pupillometric study. PLoS One 1–29.

Striem-Amit, E., Almeida, J., Belledonne, M., Chen, Q., Fang, Y., Han, Z., et al., 2016. Topographical functional connectivity patterns exist in the congenitally, prelingually deaf. Sci. Rep. 6, 29375.

Stropahl, M., Chen, L., Debener, S., 2017. Cortical reorganization in postlingually deaf cochlear implant users : intra-modal and cross-modal considerations. Hear. Res. 343, 128–137.

Thissen, D., Steinberg, L., Kuang, D., 2016. Quick and easy implementation of the Benjamini- hochberg procedure for controlling the false. J. Educ. Behav. Stat. 27, 77–83.

Tillein, J., Hubka, P., Kral, A., 2016. Monaural congenital deafness affects aural dominance and degrades binaural processing. Cerebr. Cortex 1762–1777.

Tzourio-Mazoyer, N., Landeau, B., Papathanassiou, D., Crivello, F., Etard, O., Delcroix, N., et al., 2002. Automated anatomical labeling of activations in SPM using a macroscopic anatomical parcellation of the MNI MRI single-subject brain. Neuroimage 15, 273–289.

Vrba, J., Robinson, S., 2001. Signal processing in magnetoencephalography. Methods 271, 249–271.

Wie, O.B., 2010. Language development in children after receiving bilateral cochlear implants between 5 and 18 months. Int. J. Pediatr. Otorhinolaryngol. 74, 1258–1266.

Wilke, M., Holland, S.K., Altaye, M., Gaser, C., 2008. Template-O-Matic: a toolbox for creating customized pediatric templates. Neuroimage 41, 903–913.

Wilson, B.S., 2008. Cochlear implants: current designs and future possibilities. J. Rehabil. Res. Dev. 45, 695–730.

Wong, D., Miyamoto, R.T., Pisoni, D.B., Sehgal, M., Hutchins, G.D., 1999. PET imaging of cochlear-implant and normal-hearing subjects listening to speech and nonspeech. Hear. Res. 132, 34–42.

Wong, D.D.E., Gordon, K.A., 2009. Beamformer suppression of cochlear implant artifacts in an electroencephalography dataset. IEEE Trans. Biomed. Eng. 56, 2851–2857.

Zalesky, A., Fornito, A., Bullmore, E.T., 2010. Network-based statistic: identifying differences in brain networks. Neuroimage 53, 1197–1207.

Zatorre, R.J., Belin, P., Penhune, V.B., 2002. Structure and function of auditory cortex: music and speech. Trends Cogn. Sci. 6, 37–46.